JOURNAL OF COMPUTATIONAL PHYSICS 7, 409–434 (1971)

A Monte Carlo Study of the Thermodynamic Properties of "Hard Hexagons" on the Triangular Lattice

DWAYNE A. CHESNUT*

Shell Oil Company, Denver, Colorado

Received October 26, 1970

A Monte Carlo method, developed originally to calculate thermodynamic properties in a grand canonical ensemble of lattice systems containing molecules which have finite mutual *attractions*, has been modified for studying lattice systems in which the intermolecular potential is an infinite *repulsion*. The grand ensemble formulation is reviewed briefly, and equations are given for a specific choice of transition probabilities defining a Markov process with a stationary distribution which is identical to the probability distribution of states in the grand ensemble. Results are presented for "hard hexagons" on the two-dimensional triangular lattice. For hexagons of a size that prevents simultaneous occupation of a pair of nearest-neighbor sites by two molecules, the results indicate a possible second-order phase transition for $\mu/kT \approx 2.3$ at a density around 82 % of the close-packed density. The existence, nature, and location of this transition have been more firmly established by Runnels and Combs, and by Gaunt, using other techniques. For larger hexagons excluding simultaneous second-neighbor occupancy, an apparent first-order transition occurs at $\mu/kT \approx 1.68$, with "fluid" and "solid" densities of about 69 % and 77 % of the close-packed density. These results agree, except for the effects of finite lattice size, with those extrapolated by Orban and Bellemans from exact calculations for semi-infinite lattices. When third neighbors are excluded also, the Monte Carlo results give no indication of a transition. However, Orban and Bellemans have estimated that the transition in this case occurs at $\mu/kT \approx 4.6$, well above the value (about 3.0) where convergence of this particular Monte Carlo method becomes too slow for practical use.

1. INTRODUCTION

During the past fifteen years, much effort has been devoted to calculating the thermodynamic properties of molecular systems, such as hard spheres and hard discs, for which the intermolecular pair potential is infinite over a short range of the distance separating the pair, and is identically zero at larger distances. Interest in these simple models lies primarily in the realization that the basic obstacles which

* Honorarium Teacher, Department of Mathematics, University of Colorado Denver Center, Denver, Colorado.

still prevent a complete theoretical understanding of nonideal fluids reside in the purely statistical problems connected with calculating an accurate description of average behavior for *any* assembly of interacting particles. Thus, it has become common practice to construct a "caricature" of real molecules which provides a mathematical or computational advantage while retaining, in some sense, those features of physical reality in which one is particularly interested (e.g., the occurrence of phase transitions). One always hopes that this simplification will allow the use of analytical methods, either exact or comprising a well-defined sequence of successive approximations, which will be powerful enough to yield quantitative solutions to the statistical problems. Also of interest is the growing body of evidence suggesting that some of the essential features of real fluid-solid phase transitions are more nearly duplicated by accurate calculations for these hard-core potentials than by approximate theories using more realistic potentials.

An even simpler model is obtained if one replaces a system whose molecular coordinates vary continuously with one in which the molecules can occupy only discrete points in space, thus constructing a "lattice-gas" analog of the original "continuum" system. Since any computer is limited to a finite number of significant figures for representing molecular coordinates, all computer experiments, such as the Monte Carlo [1–11] and molecular dynamics [12–18] studies, are really lattice-gas calculations, but the lattice spacing is extremely small compared to the size of the molecular hard core, which typically spans about 10^8 sites. We are concerned here with making this simplification much more extreme (so that the core spans only a small number of sites) by *formulating* the problem in terms of a lattice model. One can then use computational tricks peculiar to lattice systems which allow sampling of molecular configurations at rates perhaps two orders of magnitude faster than one can attain for "continuum" models with a given computer.

In Section 2, the particular type of hard-core models considered is described, as well as the specific case of the two-dimensional triangular lattice used for all the numerical results presented in Section 4.

Section 3 presents the considerations involved in choosing an ensemble for the Monte Carlo calculations and summarizes the grand ensemble formualtion used. The particular Markov process chosen is defined by giving its transition probabilities. Finally, the thermodynamic functions considered are expressed in terms of averages over a Markov chain realization.

Results are presented and discussed in Section 4 for three hard-core models on the triangular lattice, with the hard core large enough to exclude simultaneous occupancy of first-, second-, and third-neighbor pairs of lattice sites, respectively. These models have also been studied by Gaunt [19], Runnels and Combs [20], and by Orban and Bellemans [21]. Consideration of all the available data, including the Monte Carlo results presented here, supports the conclusions that the first-

neighbor model has a "second-order" phase transition with an infinite compressibility and that the second-neighbor model has a first-order transition. No transition is indicated for the third-neighbor model, probably because it occurs at a higher density than could be studied with the particular Monte Carlo procedure described in Section 3.

2. Hard-Core Lattice Gas Models

Consider any regular lattice containing B lattice sites. The center of each molecule contained in the lattice system must coincide with a lattice site. A model with Q-th *neighbor repulsion* is defined as follows: Suppose a molecule is on site s_0. Then no other molecule can occupy s_0 or any of its 1-st, 2-nd,..., Q-th neighbors, but the $(Q + 1)$-st and all higher-order neighbors of s_0 may be occupied. This restriction is accomplished by associating an infinite potential energy with a pair of molecules whose centers are on two sites which are neighbors of order Q *or less*; otherwise, the potential energy is zero. By convention $Q = 0$ is the "ideal" lattice-gas in which molecules cannot occupy the same lattice sites but do not otherwise interact. Notice that this does not really define a shape for the *molecule*; only the shape of the exclusion "volume" is prescribed by this recipe. Also, this is not a general hard-core lattice model (one can easily think of examples, such as dimers on the quadratic lattice, which do not fit within this framework), but this choice provides the greatest computational advantage. It should also behave more like hard discs or hard spheres than will models having irregularly shaped exclusion volumes.

Numerical results are presented in this paper only for the two-dimensional triangular lattice. Example configurations for $Q = 1$, 2, and 3 are shown in Figs. 1–3, respectively. In Figs. 1–3, the molecules are represented by shaded hexagons. These figures also illustrate the rectangular unit cell used in the Monte Carlo calculations. For each case, an almost square area can be constructed, by appropriate choice of the number of unit cells (m, n) along the two primitive vectors of the lattice. This will minimize "surface" effects, as well as making these effects conform as closely as possible to molecular dynamics [18] and Monte Carlo [11] calculations for hard discs. For the usual reason that they furnish maximum computational simplicity, periodic boundary conditions have been imposed in all calculations described below.

Although the molecules have been represented in Figs. 1–3 as "hard hexagons", this interpretation is not unique and may even be misleading since it could lead to an erroneous conclusion regarding the limiting particle shape as more and more neighbor sites are excluded. The central question is whether the thermodynamic properties of the lattice model will approach a continuum limit of hard discs or

of parallel hard hexagons. The construction used for drawing the hexagons characterized by a Q-th neighbor repulsion depends upon the coordination number of the $(Q + 1)$-st neighbor shell, Z_{Q+1}. For $1 \leqslant Q \leqslant 18$, Z_Q is either 6 or 12. When $Z_{Q+1} = 6$, the hexagon sides are formed by the perpendicular

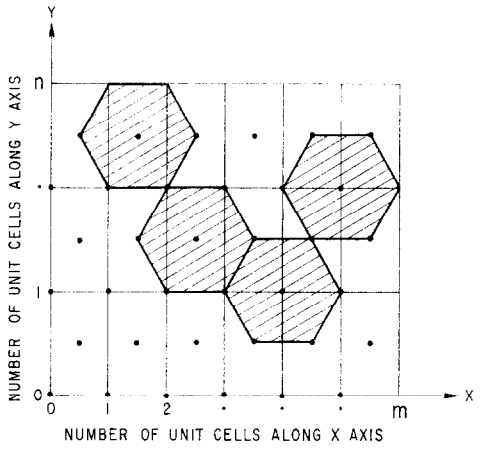

FIG. 1. "Hard-Hexagon" lattice gas with first-nearest neighbor infinite repulsion. Molecules are represented by the shaded hexagons. The small rectangles are the unit cells used for the two-dimensional triangular lattice, and the dots represent lattice sites. Each cell contains two sites: One at its lower left-hand corner, and one at its center.

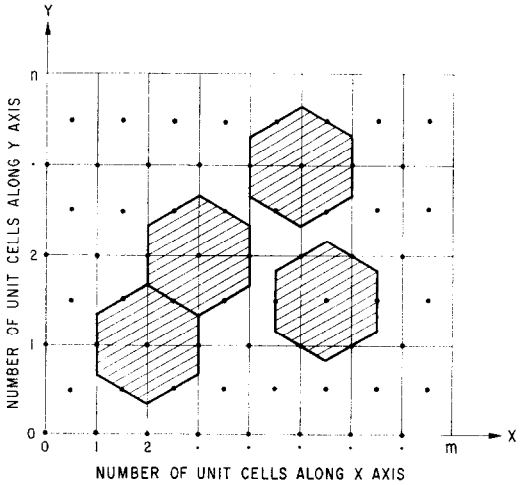

FIG. 2. "Hard-Hexagon" lattice gas with second-nearest neighbor infinite repulsion (see also the caption of Fig. 1).

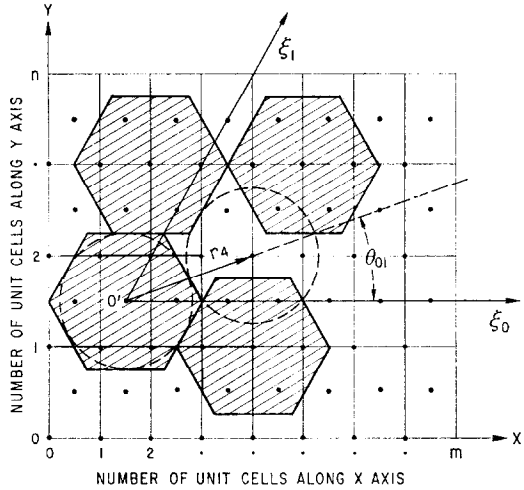

FIG. 3. "Hard-Hexagon" lattice gas with third-nearest neighbor infinite repulsion (see also the caption of Fig. 1). The auxiliary coordinate system (with origin 0′ and axes ξ_0 and ξ_1) shows the construction described in Section 2 for replacing the representation of molecules as hexagons by a representation as hard discs excluding the same neighboring sites. The two dashed circles give two examples of hard-disc molecules and show the first step in generating an infinite close-packed configuration with a molecule at the origin. The diameter of the circles is equal to the magnitude of the vector $\mathbf{r}_4$, which begins at the origin and extends to the 4th neighbor site nearest the positive ξ_0 axis.

bisectors of lines joining a central site with its 6 $(Q+1)$-st neighbors. For $Z_{Q+1} = 12$, all 12 lines joining the central site with the 12 $(Q+1)$-st neighbors are drawn, and their midpoints are marked. These lines will naturally form six pairs if one takes as pairs those lines enclosing the smallest angle. The midpoints of the two lines in each pair are then connected and extended until all the extensions intersect, thus forming a hexagon. This prescription would, of course, require modification for $Z_{Q+1} \neq 12$ or 6. A modification is unnecessary, however, because the attempt to represent molecules as hexagons breaks for another reason at $Q = 10$, when $Z_{Q+1} = Z_{11} = 6$.[1] A correct representation can always be obtained by regarding the molecules as hard discs whose centers are restricted to lattice points. Consider a close-packed array of hard discs with diameter σ, and set σ

[1] The interested reader can easily satisfy himself, with the aid of a few sheets of isometric graph paper, that the recipe described above will generate hexagonal molecules which correctly represent the Q-th neighbor repulsion for $Q < 10$. "Correct representation" here means that the molecules must have an exclusion shell containing all sites which are neighbors of order Q or less but *no others*. For $Q = 10$, two hexagons constructed according to the given rules could not occupy 12-th neighbor sites.

equal to r_{Q+1}, the $(Q + 1)$-st neighbor distance for the desired triangular lattice. This defines the spacing of the underlying triangular lattice in terms of σ.

The orientation of the triangular net can be specified by the following recipe. Consider the usual triangular coordinate system ξ_0, ξ_1 with an angle $\pi/3$ included between the axes in the positive direction. Let $\mathbf{r}_{Q+1}$ be the vector (of length σ) from the origin 0 to the $(Q + 1)$-st neighbor site of 0 which is nearest the positive ξ_0 axis. Let θ be the positive angle that $\mathbf{r}_{Q+1}$ makes with ξ_0.[2] Note that $0 \leqslant \theta < \pi/3$. If there are 6 $(Q + 1)$-st neighbors, then $\theta = 0$. The close-packed configuration of discs can be generated by placing their centers on the 6 $(Q + 1)$-st neighbor sites which can be reached by vectors of length σ at angles $\theta + (n\pi/3)$, $n = 0, 1, 2, 3, 4, 5$. Thus, it is possible to completely determine the underlying triangular lattice for a given disc diameter σ, or, given the lattice, to choose σ in such a way that a pair of discs cannot occupy neighbor sites of order Q or less but $(Q + 1)$-st, $(Q + 2)$-nd... neighbor pairs can be occupied. Since this is exactly the pair potential used above to define the hard-core model, this model is properly regarded as a numerical integration procedure for approximating the continuum model of hard discs rather than of parallel hard hexagons even though *either* interpretation is valid for sufficiently small Q.

3. Monte Carlo Procedure for The Hard-Core Lattice Model

Choice of Ensemble

Previous Monte Carlo studies of lattice models have used the petit canonical ensemble [22], the isothermal-isobaric ensemble [23, 24], and the grand canonical ensemble [25, 26] for systems of molecules interacting with a pair potential which is infinite only when two molecules occupy the same lattice site but is otherwise finite or zero. In the petit ensemble the average configurational energy and heat capacity can be obtained for such potentials in a straightforward way. However, the calculation of properties of greater interest in the study of phase transitions (e.g., the pressure p and the chemical potential μ) has so far been possible only through the computation of an average which gives estimates for the canonical partition function as a function of the number of molecules (N) and the number of lattice sites (B) at fixed thermodynamic temperature (T). These estimates can then be differentiated numerically with respect to B and N according to standard statistical thermodynamic relations to obtain approximate values of p and μ [22, 27]. Since the estimate for the partition function is very poorly behaved at best and even fails to converge for moderately large B, this indirect procedure is not very useful. To make matters still worse, the numerical method breaks down

[2] The coordinates and the construction for $Q = 3$ are illustrated by Fig. 3.

even in principle for molecules with a finite hard core, and, since there is no configurational energy for the hard-core lattice models described in Section 2, no existing Monte Carlo procedure for the petit ensemble gives *any* thermodynamic information in the form of direct averages. Current Monte Carlo methods for estimating the petit ensemble equation of state for "continuum" models cannot be extended in any obvious way for application to lattice gases because these methods employ the virial theorem, and no definition of a virial is known for lattices. Thus, a completely new approach[3] is required before useful calculations can be performed for hard-core lattice gases in the petit ensemble. By contrast, considerable thermodynamic information can be obtained from the grand canonical ensemble without a knowledge of the grand partition function, and the Monte Carlo procedure previously described in Ref. [25] can be applied to hard-core lattice gases with few changes. For these reasons we now turn our attention to the grand ensemble.

Grand Ensemble Formulation

Although the notation introduced in Ref. [25] could be used here, some simplification results from the use of a slightly different notation which is more appropriate for the hard-core models. A linear index s ($s = 0, 1, \ldots, B-1$) is assigned to the lattice sites. In a given state $\mathbf{k}$ each of the B sites may be empty or it may be occupied by the center of any one of $N_{\mathbf{k}}$ indistinguishable molecules, subject to the restrictions given below. A state $\mathbf{k}$ of the system is uniquely determined by the lattice occupation vector $\mathbf{L}(\mathbf{k})$:

$$\mathbf{L}(\mathbf{k}) = \| l_s(\mathbf{k}) \|, \tag{1}$$

where $l_s(\mathbf{k}) = 1$ if, in state $\mathbf{k}$, site s is occupied by the center of a molecule and is equal to zero otherwise. $N_{\mathbf{k}}$ denotes the number of molecules in state $\mathbf{k}$ and is given by

$$N_{\mathbf{k}} = \sum_{s=0}^{B-1} l_s(\mathbf{k}). \tag{2}$$

Allowing the elements $l_s(\mathbf{k})$ to assume only the values 0 or 1 ensures that the center of at most one molecule will be on a given lattice site. Accessible states must also satisfy the additional restriction imposed by the finite hard core of the molecules, which is conveniently formulated as follows: For $1 \leqslant q \leqslant Q$, the symmetric $B \times B$ matrices $Z^{(q)}$ are defined by

$$\mathbf{Z}^{(q)} = \| z_{ss'}^{(q)} \|, \tag{3}$$

[3] One possibility is to develop a Monte Carlo procedure based on a formulation given by B. Widom, *J. Chem. Phys. 39* (1963), 2808 and also by Klein and Jackson, *Phys. Fluids 7* (1964), 2281 relating the chemical potential to the "potential energy distribution" of a fluid. This might be a promising approach for lattice models.

where $z_{ss'}^{(q)} = 1$ if sites s and s' are q-th neighbors and is equal to zero otherwise. The $\mathbf{Z}^{(q)}$ are then combined to form the symmetric $B \times B$ exclusion matrix $\mathbf{E}^{(Q)}$ for Q-th neighbor repulsion:

$$\mathbf{E}^{(Q)} = \bigcup_{q=1}^{Q} \mathbf{Z}^{(q)} = \| e_{ss'}^{(Q)} \|, \tag{4}$$

where $\bigcup_{q=1}^{Q}$ represents the logical union of the $\mathbf{Z}^{(q)}$, element by element. Note that $e_{ss'}^{(Q)}$ is either zero or one; if $e_{ss'}^{(Q)} = 0$, both s and s' *may* be occupied and if $e_{ss'}^{(Q)} = 1$, at most one of the pair s, s' can be occupied. Then the *only* accessible states $\mathbf{k}$ are those for which

$$\Omega_{\mathbf{k}} \equiv \mathbf{L}(\mathbf{k}) \cdot \mathbf{E}^{(Q)} \cdot \tilde{\mathbf{L}}(\mathbf{k}) = 0, \tag{5}$$

where $\tilde{\mathbf{L}}$ denotes the transpose of $\mathbf{L}$. For configurations having a nonzero value of $\Omega_{\mathbf{k}}$, two or more molecules overlap to give an infinite potential energy and hence a Boltzmann weight of zero.

The grand partition function Ξ_B for the hard-core lattice gas is defined by

$$\Xi_B(\beta\mu, B) = \sum_{\mathbf{k}} \delta_{0,\Omega_{\mathbf{k}}} \exp(\beta\mu N_{\mathbf{k}}), \tag{6}$$

where μ is the chemical potential per molecule, $\beta = (kT)^{-1}$, k is the Boltzmann constant, T is the thermodynamic temperature, and $\delta_{0,\Omega_{\mathbf{k}}}$ is the Kronecker delta. The probability that a system selected at random from the grand ensemble will be in state $\mathbf{k}$ is then

$$P_{\mathbf{k}}(\beta\mu, B) = \Xi_B^{-1} \delta_{0,\Omega_{\mathbf{k}}} \exp(\beta\mu N_{\mathbf{k}}), \tag{7}$$

and the grand ensemble average $\langle y \rangle$ for a state function $y(\mathbf{k})$ is

$$\langle y \rangle = \sum_{\mathbf{k}} P_{\mathbf{k}} y(\mathbf{k}). \tag{8}$$

We shall also make use of the density function,

$$P_N(\beta\mu, B) = \sum_{\mathbf{k}} P_{\mathbf{k}}(\beta\mu, B)\, \delta_{N,N_{\mathbf{k}}}, \tag{9}$$

which gives the probability of selecting a system containing exactly N molecules from the grand ensemble.

The Markov Process

The reader who is not already familiar with the general features of Monte Carlo methods, as used in statistical mechanics, may wish to consult a previous paper by Wood and Parker [28] for a more complete discussion of its theoretical basis. Only a brief description will be given here. In statistical mechanical applications, one first constructs a stochastic matrix $\| P_{\mathbf{jk}} \|$ defining a discrete-time finite Markov process (or chain) which has the desired ensemble density function

as its stationary distribution. Element $P_{\mathbf{jk}}$ represents the probability that a transition from state $\mathbf{j}$ to state $\mathbf{k}$ will occur at any particular single step of the chain. A digital computer is then used to develop a *realization* of this Markov chain, i.e., a particular sequence of $W + 1$ states $\mathbf{k}(0)$, $\mathbf{k}(1)$,..., $\mathbf{k}(t)$,..., $\mathbf{k}(W)$. The arbitrary initial state is $\mathbf{k}(0)$; succeeding states are generated according to the $P_{\mathbf{jk}}$ by appropriate use of pseudorandom number sequences. The average of any state function $y(\mathbf{k})$ can be written as

$$\bar{y} = (W - \tau + 1)^{-1} \sum_{t=\tau}^{W} y[\mathbf{k}(t)]. \tag{10}$$

It is computed for the realization (where the averaging process is initiated at step $\tau \geqslant 1$) and converges stochastically (for any fixed τ) as $W \to \infty$ to the corresponding ensemble average $\langle y \rangle$. An estimate for the variance of $\bar{y}$ can be obtained by noting that the realization of total length W may be considered as a set of consecutive subrealizations of fixed arbitrary length ΔW. The function $y(\mathbf{k})$ is averaged separately over each subrealization to produce a sequence of subchain averages that become statistically independent and normally distributed if ΔW is "large enough". The subchain averages may therefore be processed by familiar statistical methods for small samples to estimate the variance of $\bar{y}$.

For our present purposes we require a Markov process which has the grand ensemble density function $P_{\mathbf{k}}$, given by Eq. (7), as its stationary distribution. As usual, one can construct a variety of such processes, and the choice of a particular one is largely arbitrary. The results described later (Section 4) were obtained from Markov chain realizations generated according the following transition probabilities:

$$\begin{aligned} P_{\mathbf{jk}} &= B^{-1}\,\delta_{0,\Omega_{\mathbf{k}}}, \qquad \text{for} \quad \beta\mu(\Delta N)_{\mathbf{jk}} \geqq 0, \qquad \mathbf{k} \neq \mathbf{j} \\ &= B^{-1}\,\delta_{0,\Omega_{\mathbf{k}}} \exp\{\beta\mu(\Delta N)_{\mathbf{jk}}\}, \qquad \text{for} \quad \beta\mu(\Delta N)_{\mathbf{jk}} < 0, \qquad \mathbf{k} \neq \mathbf{j}; \\ P_{\mathbf{jj}} &= -\sum_{\mathbf{k} \neq \mathbf{j}} P_{\mathbf{jk}}\,. \end{aligned} \tag{11}$$

Equations (11) hold for distinct pairs of states (i.e., $\mathbf{j} \neq \mathbf{k}$) such that $l_s(\mathbf{j}) = l_s(\mathbf{k})$ for all s except $s = s_0$ ($0 \leqslant s_0 \leqslant B - 1$), and $l^c_{s_0}(\mathbf{j}) = l_{s_0}(\mathbf{k})$, where $l^c_{s_0}$ is the logical complement of l_{s_0}. For all other pairs of distinct states $P_{\mathbf{jk}} = 0$. The definition of $P_{\mathbf{jj}}$ ensures that these transition probabilities are normalized, and it is a trivial excercise to show that they satisfy the "microscopic reversibility" condition $P_{\mathbf{j}}P_{\mathbf{jk}} = P_{\mathbf{k}}P_{\mathbf{kj}}$ for the grand ensemble. Furthermore, the states all belong to the same ergodic class (at least for finite $\beta\mu$ and B): A finite sequence of steps having a nonzero multistep transition probability can be constructed which connects any pair of allowed states. The sequence may, however, be quite long with a very small multistep probability for some pairs. Hence, the stochastic matrix given by Eq. (11)

satisfies all the conditions sufficient [11, 28] to define a Markov process which converges to the grand ensemble distribution, Eq. (7). We shall now summarize the use of Markov chain averages for several specific state functions in estimating thermodynamic properties.

Thermodynamic Functions

The stochastic matrix defined by Eqs. (11) is fixed by choosing values for the parameters B, Q, and $\beta\mu$. The number of molecules will, in general, vary from one step to the next in a Markov realization, as discussed below (Section 4) in describing the computer implementation of this procedure. The state functions N_k, N_k^2, N_k^3 and δ_{N,N_k} can be averaged over a chain realization of length W by using Eq. (10). For finite W, these chain averages provide estimates for the corresponding grand ensemble averages: $\langle N\rangle$, $\langle N^2\rangle$, $\langle N^3\rangle$, and P_N, where P_N is given by Eq. (9).

From the first three of these averages, one can estimate the following thermodynamic functions:

$$\langle \rho^* \rangle = (N_M)^{-1}\langle N\rangle, \tag{12}$$

$$(\partial\langle \rho^* \rangle/\partial\beta\mu)_B = (N_M)^{-1}[\langle N^2\rangle - \langle N\rangle^2] \tag{13}$$

and

$$(\partial^2\langle \rho^* \rangle/\partial(\beta\mu)^2)_B = (N_M)^{-1}[\langle N^3\rangle - 3\langle N^2\rangle\langle N\rangle + 2\langle N\rangle^3], \tag{14}$$

where N_M is the number of molecules at close packing. Equation (12) defines a reduced density $\langle \rho^* \rangle$ which is the lattice-gas analog for the reciprocal of the reduced volume commonly used in studies of hard spheres and discs. Equations (13) and (14) for the first and second derivatives, respectively, of $\langle \rho^* \rangle$ with respect to $\beta\mu$ at constant B follow from standard grand ensemble fluctuation theory [27]. Although Q is also understood to be held fixed in evaluating these partial derivatives, this is not indicated by the usual subscript notation since it is not a thermodynamic variable.

The estimate of P_N obtained from the Markov chain realizations is of interest for two reasons. First of all, this function can be renormalized by the relation

$$P(\rho^*) = N_M P_N \tag{15}$$

to obtain the probability $P(\rho^*)\,\Delta\rho^*$ of observing a system in the grand ensemble with a reduced density within $\Delta\rho^*$ of ρ^*. When the thermodynamic variables are given values corresponding to a single-phase region, $P(\rho^*)$ will be a sharply peaked function having a unique maximum for a sufficiently large finite system and will become a Dirac delta in the thermodynamic limit. In a two-phase region, however, a bimodal $P(\rho^*)$ may be expected for a large enough finite system, and the existence of two maxima in $P(\rho^*)$ represents a qualitative finite-system manifestation of a

first-order phase transition in the corresponding infinite system [29] (see also Ref. [27, Appendix 9]). In the second place, note that P_N can be written in the form

$$P_N = \Xi_B^{-1} Q_N(B) \exp(\beta\mu N), \tag{16}$$

since the sum over $\mathbf{k}$ at fixed N of $\delta_{0,\Omega_\mathbf{k}}$ is just the definition for the lattice-gas petit ensemble configurational partition function $Q_N(B)$. If N is so large that for all practical purposes it may be regarded as a continuous variable, the canonical ensemble chemical potential can be defined by

$$\beta\hat{\mu}(N) = -\left(\frac{\partial \ln Q_N}{\partial N}\right)_B. \tag{17}$$

For small systems, define $\beta\hat{\mu}$ by replacing the derivative in (17) by its finite-difference analog: $\frac{1}{2}\ln[Q_{N+1}/Q_{N-1}]$. This in turn can be expressed in terms of $\ln P_N$ with the aid of (16). Then, because the Markov chain average $\omega_N(\beta\mu) \equiv \delta_{N,N_\mathbf{k}}$ converges to P_N one can take

$$\beta\hat{\mu} = \beta\mu - \tfrac{1}{2}\ln[\omega_{N+1}/\omega_{N-1}] \tag{18}$$

as an estimate of the canonical ensemble chemical potential. Thus, the grand ensemble Monte Carlo procedure outlined here can be used to study the "Van der Waals' loop" which is generally expected in the canonical ensemble as a finite-system manifestation of a first-order phase transition, since a bimodal P_N will obviously give such a loop.

Generation of the Markov Chain

Let us now consider the generation of a single step in the Markov chain, i.e. a transition from state $\mathbf{j}$ to state $\mathbf{k}$, where the probabilities for all pairs of states $\mathbf{j}$, $\mathbf{k}$ are defined by Eqs. (11). A site number s_0, between 0 and $B - 1$, is selected, with probability B^{-1}, by multiplying B by a pseudorandom fraction f_1. This fraction is generated from the Lehmer multiplicative pseudorandom sequence described by Taussky and Todd [30]. Numbers in this sequence exhibit many of the properties of random samples from a uniform distribution on the interval (0, 1). Site s_0 is then examined to determine whether it is empty or occupied.

If site s_0 is *empty* in state $\mathbf{j}$, a molecule is tentatively placed on s_0 to generate a trial state $\mathbf{k}$. This trial configuration is then checked for overlap between the added molecule and those already on the lattice. If an overlap is found, the trial state is rejected, and state $\mathbf{j}$ is retained as the next step in the chain.

Otherwise, acceptance or rejection of state $\mathbf{k}$ depends on the sign of the quantity $\beta\mu(N_\mathbf{k} - N_\mathbf{j})$, which in this case is equal to $\beta\mu$ (since $N_\mathbf{k} - N_\mathbf{j} = +1$).

For $\beta\mu \geqslant 0$, state $\mathbf{k}$ is accepted as the next step in the chain, and the lattice configuration is updated.

If $\beta\mu < 0$, a random fraction f_2 is generated from an additive pseudorandom sequence described and extensively tested for "randomness" by Green, Smith, and Klem [31], and compared with $\exp(-|\beta\mu|)$. If $f_2 \leqslant \exp(-|\beta\mu|) \equiv \exp(\beta\mu)$, state **k** is accepted and the lattice configuration is updated. Otherwise, state **k** is rejected and state **j** is retained as the next step in the chain.

Next, consider the case that site s_0 is *occupied*. The trial state **k** is then generated by tentatively *removing* the molecule from s_0, and there is no possibility of creating an overlap. Acceptance or rejection of **k** thus depends entirely on the quantity $\beta\mu(N_k - N_j)$, which is equal to $-\beta\mu$ because $N_k - N_j = -1$.

If $\beta\mu \leqslant 0$, state **k** is accepted as the next step in the chain, and the lattice configuration is updated.

For $\beta\mu > 0$, a pseudorandom fraction f_2 is generated from the additive sequence described above and compared with $\exp(-|\beta\mu|) \equiv \exp(-\beta\mu)$. If $f_2 \leqslant \exp(-\beta\mu)$, state **k** is accepted and the necessary updating is performed. Otherwise, state **j** is retained as the next step in the chain.

Note that, when $\beta\mu > 0$, discrimination on the Boltzmann factor is required only when attempting to *remove* a molecule. If $\beta\mu < 0$, this discrimination is required only when attempting to *add* one. The sign of $\beta\mu$ is tested on entry to determine which of several program-modification steps are executed in the initializing sequence to eliminate superfluous tests on the sign of $\beta\mu$ from the main loop.

4. Presentation and Discussion of Results

The Monte Carlo procedure described in Section 3 was used to study the hard-core model on the two-dimensional triangular lattice for first, second-, and third-neighbor infinite repulsion. Estimates for the grand ensemble average reduced density, its standard deviation, and its first two derivatives with respect to $\beta\mu$ are given for several values of $\beta\mu$ in Table I for $Q = 1$, $B = 81$, 324, and 360; Table II for $Q = 2$, $B = 360$ and 480; and Table III for $Q = 3$, $B = 392$. All values of B were chosen so that the maximum number of molecules (N_M) which can be put on the lattice would form a regular close-packed configuration. The rectangular unit cell containing two lattice sites (see Figs. 1–3) was used with $m = 18$, $n = 10$ for $B = 360$; $m = 20$, $n = 12$ for $B = 480$; and $m = n = 14$ for $B = 392$. For $B = 81$ and 324, the customary triangular coordinate system was employed with arrays of 9×9 sites and 18×18 sites.

The petit ensemble chemical potential $\beta\hat{\mu}(\rho^*)$ was obtained by first computing estimates from the Markov chain averages $\omega_N(\beta\mu)$ [according to Eq. (18)] for each assigned value of $\beta\mu$, B, and Q. All the estimates for each fixed B and Q at a given N (and thus ρ^*) were then weighted by $W^{1/2}N_M\omega_N(\beta\mu)$, discarding all estimates for

which $N_M\omega_N(\beta\mu) < 0.5$, to obtain weighted averages and standard deviations.[4] This averaging procedure, although arbitrary, is based upon the qualitative considerations that the overall precision of any average over a Markov chain realization increases in proportion to $W^{1/2}$, while the best estimates of any function of ω_N will be obtained in a region around the maximum of $P(\rho^*)$ where the Markov chain sampling is best. Ideally, one would prefer an estimate of the error in $\beta\hat{\mu}$ for each Markov chain realization, but this appears to require a statistical analysis of a complexity comparable to that used by W. W. Wood in his study of hard discs [6] and it is doubtful whether the error estimate for $\beta\hat{\mu}$ would be sufficiently

81 — SITE LATTICE				
0.00	0.4881 ± 0.0009	0.132	—	0.4
0.50	0.5487 ± 0.0021	0.121	—	0.6
1.00	0.6042 ± 0.0021	0.119	—	0.6
1.50	0.6723 ± 0.0024	0.157	—	4.4
2.00	0.7740 ± 0.0057	0.254	—	4.2
2.50	0.8754 ± 0.0075	0.188	—	3.0
324 — SITE LATTICE				
2.05	0.7338 ± 0.0033	0.170	—	5.2
2.25	0.7992 ± 0.0039	0.301	—	9.8

[4] Tables of these weighted averages are available from the author on request.

TABLE II

Grand Ensemble Averages, as a function of Chemical Potential, for the Hard Hexagon Lattice Gas With Second-Neighbor Repulsion

$\beta\mu$	$\langle\rho^*\rangle$	$\partial\langle\rho^*\rangle/\partial(\beta\mu)$	$\partial^2\langle\rho^*\rangle/\partial(\beta\mu)^2$	$10^{-6}W$
360 — SITE LATTICE				
1.25	0.5849 ± 0.0013	0.172	0.277	8
1.50	0.6475 ± 0.0022	0.363	1.406	20
1.60	0.7038 ± 0.0028	0.552	0.850	24
1.64	0.7189 ± 0.0023	0.565	0.220	36
1.65	0.7300 ± 0.0029	0.572	−0.325	24
1.70	0.7548 ± 0.0029	0.518	−0.954	20
1.75	0.7814 ± 0.0026	0.450	−1.290	20
2.00	0.8572 ± 0.0015	0.192	−0.491	12
2.20	0.8906 ± 0.0006	0.119	−0.157	12
2.25	0.8950 ± 0.0007	0.117	−0.202	16
480 — SITE LATTICE				
1.65	0.7182 ± 0.0027	0.625	0.684	25.2
1.66	0.7266 ± 0.0028	0.670	−1.952	25
1.67	0.7160 ± 0.0027	0.626	1.095	29.6
1.68	0.7147 ± 0.0022	0.625	1.423	38.4

TABLE III

Grand Ensemble Averages, as a Function of Chemical Potential, for the Hard Hexagon Lattice Gas With Third-Neighbor Repulsion

$\beta\mu$	$\langle\rho^*\rangle$	$\partial\langle\rho^*\rangle/\partial(\beta\mu)$	$\partial^2\langle\rho^*\rangle/\partial(\beta\mu)^2$	$10^{-6}W$
392 — SITE LATTICE				
0.00	0.5304 ± 0.0002	0.094	−0.018	7.8
1.00	0.6165 ± 0.0002	0.078	−0.016	20.8
1.60	0.6606 ± 0.0006	0.071	−0.010	8.6
2.00	0.6886 ± 0.0008	0.066	−0.012	6.4

($Q = 0$) for comparison. Since Fig. 4 is intended to show just the overall qualitative features of the Monte Carlo results, it includes only the canonical ensemble chemical potentials for $Q = 1$, $B = 360$; $Q = 2$, $B = 360$; and $Q = 3$, $B = 392$, along with three grand ensemble points and slopes for $Q = 1$, $B = 81$. The remainder of the data have been omitted in order to avoid unnecessary clutter.

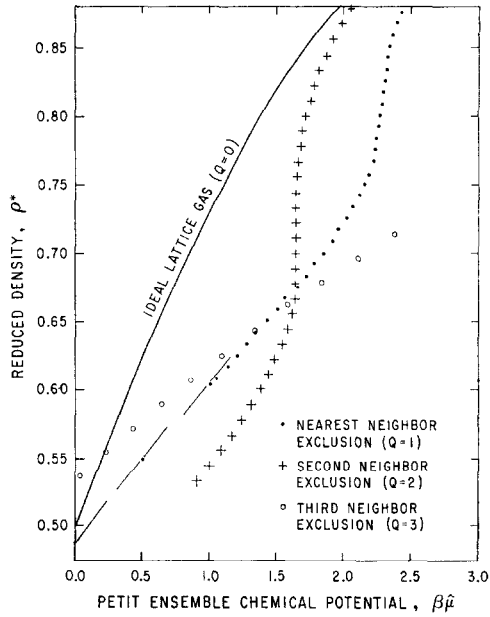

FIG. 4. Reduced density ρ^* as a function of the *petit* ensemble chemical potential $\beta\hat{\mu}$ for hard hexagon lattice gases, obtained from the *grand* ensemble Monte Carlo calculations [see Eq. (18)]. The straight line segments for the nearest-neighbor case represent *grand* ensemble estimates for the reciprocal of the derivative $\partial\langle\rho^*\rangle/\partial(\beta\mu)$. The exact curve for the ideal lattice gas, with only occupied sites excluded by the infinite repulsion, is shown for comparison.

Indications of Phase Transitions

The main point of interest in Fig. 4 is that the curves for both $Q = 1$ and $Q = 2$ (but not $Q = 3$) each indicate a possible "phase transition". In the former case this is manifested by a rather abrupt change in slope near $\rho^* = 0.75$, indicating a possible second-order transition, while in the latter case one observes an essentially vertical section of the curve beginning near $\rho^* = 0.68$, which may be a first-order transition. Since other studies confirm the existence of transitions in all three cases [19–21], it may seem odd that the third-neighbor exclusion model results do not show any indication of one. However, at the time the Monte Carlo calculations were completed, it appeared likely that the $Q = 3$ transition occured at higher densities. This was subsequently confirmed by Orban and Bellemans [21]. Unfortunately, higher densities cannot be reached with the computer programs because the Monte Carlo sampling procedure breaks down for $\beta\mu$ greater than about 3.

First-Neighbor Repulsion

A more detailed plot of the canonical chemical potential vs ρ^* in the "phase transition region" for $Q = 1$ is given in Fig. 5. As pointed out in Section 3, a

"Van der Waals' loop" in $\beta\hat{\mu}$ as a function of ρ^* is commonly regarded as the finite-system equivalent of a *first*-order phase transition [11]. While the existence of such a loop for a finite system may not always imply a first-order transition in the thermodynamic limit, its total absence in Fig. 5 strongly suggests that this "transition" is of higher order. Furthermore, none of the $P(\rho^*)$ curves for $Q = 1$ appeared to be bimodal, although relatively broad distributions were observed for each B in Table I at values of $\beta\mu$ (corresponding to densities in the "transition" region) within a small range which shifts slightly toward higher chemical potentials as B increases. The $P(\rho^*)$ curve shown in Fig. 6 for $\beta\mu = 2.20$, $B = 360$ is the broadest distribution observed for this value of B and represents a chemical potential near the center of the "phase transition" region of Fig. 5. The other two curves in Fig. 6 are more sharply peaked and provide typical examples of this function's behavior both above and below the "transition" for the 360-site lattice.

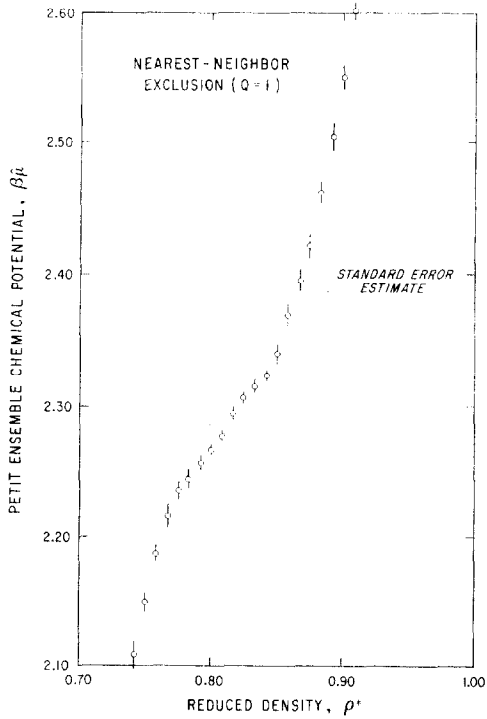

FIG. 5. Detail of the "phase transition region" for the hard-hexagon lattice gas with nearest-neighbor exclusion. Other studies indicate that the derivative $\partial(\beta\hat{\mu})/\partial\rho^*$ approaches *zero* in the thermodynamic limit at a reduced density of about 0.84, which is within the density range where the Monte Carlo results show a noticeable flattening in the plot of petit ensemble chemical potential ($\beta\hat{\mu}$) vs reduced density (ρ^*).

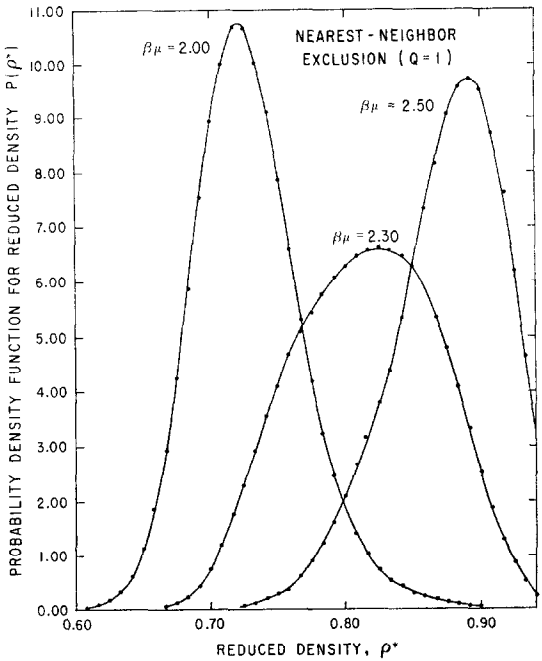

FIG. 6. Monte Carlo estimates for the probability density function $P(\rho^*)$ [see Eq. (15)] at grand ensemble chemical potentials below, within, and above the "phase transition" region of the hard-hexagon lattice gas with nearest-neighbor exclusion. The broadening of this distribution for $\beta\mu = 2.30$ is one of the observations suggesting a possible phase transition.

It seems fairly safe to conclude from these data that the first-neighbor hard-core lattice gas does *not* have a first-order transition. To go beyond this point and attempt to determine whether a transition of higher order exists necessarily becomes more speculative because the Monte Carlo data are rather limited. However, it seems worthwhile to do this for two reasons. Firstly, one might expect that the detection of a phase transition by Monte Carlo studies would be somewhat more difficult when it is not first-order and it is of interest to obtain a qualitative indication of just how difficult it may be. Secondly, in contrast to the first-order case, little is known about the behavior of Markov chain realizations for finite systems in a region where the corresponding infinite system has, say, a second-order transition, and even a crude example is interesting.

As one can see in Fig. 5, the curve for the canonical chemical potential as a function of reduced density exhibits a relatively small slope and a change from negative to positive curvature for ρ^* between approximately 0.77 and 0.85. (This is also apparent from the grand ensemble results in Table I.) The isothermal compressibility, which is essentially the reciprocal of this slope, thus becomes rather

large over a narrow range in density. Assuming that a transition exists and that it is not first order, consider two possibilities: (A) the isothermal compressibility has a finite discontinuity at some ρ^*, which corresponds to a transition of second-order in the Ehrenfest sense; or (B) the isothermal compressibility becomes infinite at some ρ^* to give a "λ-point" type of transition.

D. M. Burley [32] has studied several lattices with first-neighbor repulsions, using the Bethe and related approximations. For "loose-packed" lattices such as the two-dimensional square net (which is the most relevant lattice for our present consideration), he was able to extend both the Bethe and ring approximations so they could be used to take into account holes in a close-packed configuration and thus to get approximate high-density equations for the free energy. The usual forms of these approximations were used to obtain similar equations valid at low density. The high density solution in both approximations is the more stable (i.e., has a lower free energy) in comparison with the low density solution in the same approximation, but in both cases below a "critical density" the high density solution corresponds to imaginary values of certain physically observable quantities and thus becomes unrealizable. Furthermore, in both approximations the curves join at the "critical density" in such a way that there is a second-order transition of type (A) above with a large but finite discontinuity in the isothermal compressibility.

D. S. Gaunt and M. E. Fisher [33] used Padé approximants to extend exact

model has a second-order transition, and that the compressibility probably remains finite at the transition point. However, they could not definitely exclude the possibility of a very weak singularity, such as the logarithmic divergence of the compressibility suggested by extrapolating the exact properties of semi-infinite square lattices to obtain estimates for the corresponding thermodynamic limits [20, 34, 35]. These extrapolations provide especially convincing evidence that this model has a "λ-point" transition.

Fisher's superexchange model [36] has an infinite repulsion between nearest-neighbor molecules on the square lattice as well as a finite attraction between second-nearest neighbors on *alternate* squares. Fisher was able to derive an analytical expression at one temperature for the partition function and showed that the pressure is a continuous function of the density. However, it has a zero first derivative at $\rho_t^* \approx 0.706$, and the isothermal compressibility becomes logarithmically infinite at ρ_t^*. As $T \to \infty$, this model reduces to the simple hard square lattice gas, and Fisher speculated that the "λ-point" nature of this transition might remain essentially unchanged as T increases. This speculation now appears to be correct.

Finally, the λ-point nature of the transition for the first-neighbor hard hexagon

lattice gas was rather convincingly shown, after the Monte Carlo study was completed, by Gaunt [19], by Runnels and Combs [20], and by Orban and Bellemans [21]. Gaunt used the Padé approximant approach, and the others used what Runnels has called "exact finite methods".

The evidence is now very strong that a hard-core interaction extending to first-neighbor sites on both the triangular and the quadratic lattice produces a "continuous" or "second-order" transition and that the isothermal compressibility has a logarithmic singularity at the transition point. Thus, the isothermal compressibility for the first-neighbor case, considered as a function of density, resembles the ordinary Ising heat capacity as a function of temperature in zero field. The behavior observed by Burley is not inconsistent with this. Applying the *same* approximations he used to the two-dimensional Ising model gives finite discontinuities in the heat capacity near the critical temperature, whereas the exact solution has a logarithmic singularity at T_c. To determine whether the Monte Carlo results are consistent with this behavior, the petit ensemble chemical potential was differentiated numerically (using a centered two point difference formula) with respect to density to obtain an estimate for $(\partial\beta\hat{\mu}/\partial\rho^*)_T$. This derivative was then used in the thermodynamic relation:

$$\frac{\rho K}{\beta} = \left[\rho^* \left(\frac{\partial \beta\mu}{\partial \rho^*}\right)_T\right]^{-1}, \tag{19}$$

to estimate the quantity $\rho K/\beta$, where K is the isothermal compressibility. The results of this calculation are shown in Fig. 7, along with a few additional points obtained from the grand ensemble averages. No attempt was made to smooth the data in any way, and the scatter in the petit ensemble results is quite large, especially in the interesting region. Nevertheless, one might plausibly speculate that Fig. 7 represents an "experimental" measurement near a λ-point, even without the other evidence cited above.

The solid curve in Fig. 7 below the transition region was obtained from the following series (which is a simple rearrangement of the fugacity series):

$$\frac{(1-\rho^*)(\beta\mu - \ln\rho)}{2B_2{}^*\rho^*} = 1 + \sum_{n\geqslant 1} (2B_2{}^*)^{-1}\left[\left(\frac{n+2}{n+1}\right) B^*_{n+2} - \left(\frac{n+1}{n}\right) B^*_{n+1}\right](\rho^*)^n, \tag{20}$$

where $B_n{}^* = B_n\sigma^{-n+1}$, σ is the number of lattice sites covered by one molecule, and B_n is the n-th lattice-gas virial coefficient. The right side of (20) was then written as a continued fraction of the form

$$F(\rho^*) = 1/1 + c_1\rho^*/1 + c_2\rho^*/1 + \cdots, \tag{21}$$

and the virial coefficients through B_6 given by Burley were used to obtain c_1, c_2, c_3,

and c_4. This gives the fourth approximant $A_4(\rho^*)$ to the continued fraction expansion which can be written as the ratio of two second-degree polynomials in ρ^*. When the resulting expression is substituted for the RHS of (20), differentiation with respect to ρ^* followed by rearrangement and the use of (19) gives

$$\left(\frac{\rho K}{\beta}\right)^{-1} = 1 + 2B_2^* \left(\frac{\rho^*}{1-\rho^*}\right)\left[\rho^* \frac{dA_4(\rho^*)}{d\rho^*} + \frac{A_4(\rho^*)}{1-\rho^*}\right]. \tag{22}$$

The estimate of $\rho\,(K/\beta)$ calculated from (22) has a singularity[5] at $\rho^* \approx 0.78$ and has a qualitative similarity to the low-density Monte Carlo results. The solid curve above the transition region in Fig. 7 was obtained in a similar way by using the

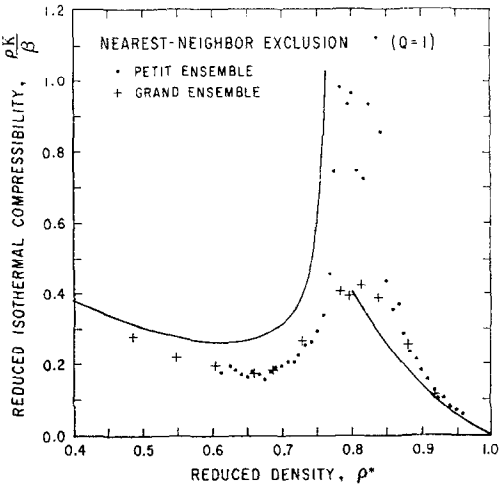

FIG. 7. Monte Carlo results for the reduced isothermal compressibility as a function of reduced density for the hard-hexagon lattice gas with nearest-neighbor exclusion. The solid curves are based on the first few terms in exact high- and low-density series expansions. The location of the maximum in both the petit and the grand ensemble results is near the estimates of Runnels and Combs, Orban and Bellemans, and Gaunt for the reduced density at the "λ-point" transition for this model.

first two coefficients in an expansion of the grand partition function as a power series in $e^{-\beta\mu}$. This estimate for $\rho(K/\beta)$ agrees well with the Monte Carlo results above $\rho^* \approx 0.92$ and has no singular behavior. However, including additional terms in this expansion would introduce a singularity.

[5] The location of this singularity is surprisingly close, considering that only 6 virial coefficients were used, to Gaunt's estimate of $\rho_i^* = 0.832 \pm 0.008$ and Runnels' estimate (0.837 ± 0.020) for the density at the transition point.

The grand ensemble estimates for $\rho(K/\beta)$, indicated by the crosses in Fig. 7, are subject to considerably less numerical uncertainty since no differentiation is required, but they exhibit only a rather unimpressive broad maximum in the transition region. This is again similar to the behavior of the Ising heat capacity for a finite system, as shown in a Monte Carlo study by C. P. Yang [24] on the square lattice. He found that, for finite systems, the Ising heat capacity has a broad maximum near T_c which becomes higher and narrower as the lattice size is increased, and that the position of the maximum shifts toward the correct critical temperature.

Second-Neighbor Repulsion

Figure 8 shows a plot of the canonical chemical potential as a function of reduced density near the phase transition for $Q = 2$, $B = 360$ and 480, and exhibits a

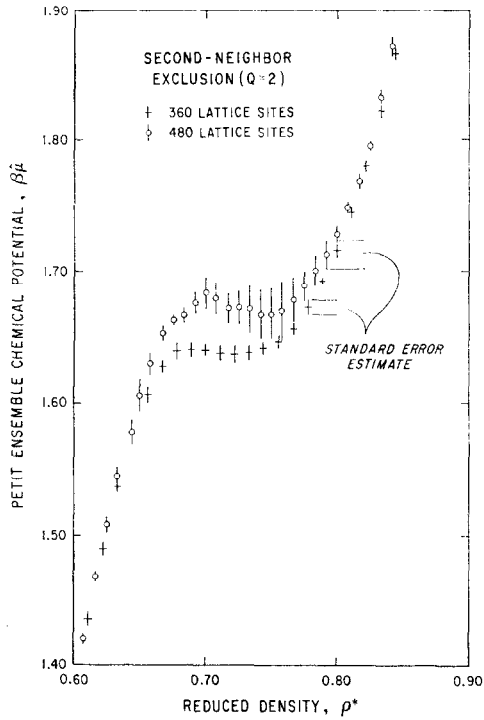

FIG. 8. Detail of the "phase transition region" for the hard-hexagon lattice gas with second-neighbor exclusion. Dependence of these Monte Carlo results on lattice size is most pronounced in the neighborhood of the "Van der Waals" loop which is probably a finite-system manifestation of a first-order phase transition in the thermodynamic limit. Orban and Bellemans' results indicate a first-order transition at $\beta\mu \approx 1.75$, with a tie-line extending from $\rho^* \approx 0.685$ to $\rho^* \approx 0.801$.

possible first-order transition for both values of B. For the smaller lattice the chemical potential is essentially constant for ρ^* between 0.68 and 0.74, while for the larger lattice the chemical potential shows a very shallow "Van der Waals' loop" (if one ignores the large error flags) between $\rho^* \approx 0.69$ and $\rho^* \approx 0.76$. Thus the density gap across the transition appears to be approximately 0.06 or 0.07, the same order of magnitude as the reduced density difference of about 0.03 which has been estimated for the hard disc transition by Alder and Wainwright and by W. W. Wood [11]. This qualitative agreement encourages one to suppose that this "transition" may indeed be essentially the same as that for hard discs (although it occurs at a different density), and hence is a probable fluid-solid type of transition.[6] It is certainly different from the first-order transition for the ordinary lattice-gas with finite *attractions* between neighboring molecules. This transition has a very much larger density gap and is therefore generally regarded as a model for the liquid-gas transition.

A rather odd feature of the results shown in Fig. 8 is the appearance of a "loop" in $\beta\hat{\mu}$ vs ρ^* for $B = 480$ but not for $B = 360$. This is somewhat unexpected since such small-system loops must (as B increases indefinitely) eventually become smaller in extent and finally disappear in the thermodynamic limit according to

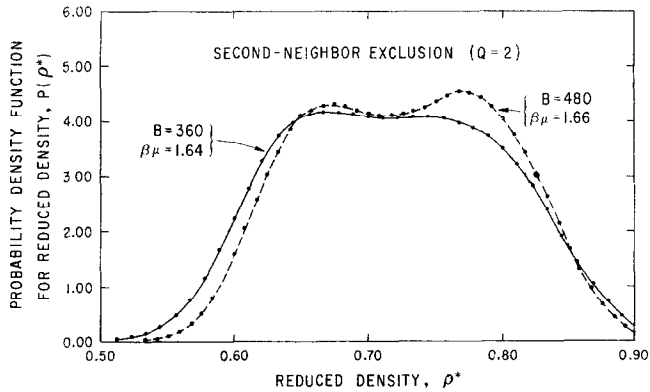

FIG. 9. Monte Carlo estimates for the probability density function $P(\rho^*)$ at grand ensemble chemical potentials within the "phase transition region" of the hard-hexagon lattice gas with second-nearest neighbor exclusion. The shape changes from a broad distribution with an essentially flat top to a bimodal distribution when the size of the lattice is increased from 360–480 sites. Thus, the finite-system indications of a first-order transition become *more* pronounced with increasing size in this size range. Similar behavior for hard discs has been reported by W. W. Wood.

[6] Orban and Bellemans have confirmed the existence of this first-order transition at $\beta\mu = 1.75 \pm 0.005$, with reduced coexistence densities of 0.685 ± 0.015 and 0.801 ± 0.005. They used an "exact finite method." The Monte Carlo results differ from theirs primarily due to small system effects.

Van Hove's theorem [37]. It is certainly possible that this is simply a numerical artifact arising from the relatively large errors in the Monte Carlo results, but this may be a real effect due to the very small size of the systems considered here. Some support for the latter view is given by the $P(\rho^*)$ curves shown in Fig. 9 for these two values of B. For the smaller lattice this distribution is quite flat with no apparent bimodal behavior while $P(\rho^*)$ for the larger lattice has two well-developed peaks. Although no explicit bounds can be given, the errors for these Monte Carlo estimates are probably considerably smaller than those for the canonical chemical potential since the numerical differentiation required to obtain $\beta\hat{\mu}$ from $P(\rho^*)$ will magnify any uncertainty. Hence, the difference between the two $P(\rho^*)$ curves and therefore the derived chemical potential curves is very likely not a numerical artifact but an apparently complicated small-system effect.

A more detailed study of the B-dependence of thermodynamic properties for this model would provide an interesting comparison with approximate macroscopic theories of a first order transition region as given by Hill and Katsura [38] and more recently by Mayer and Wood [29].

5. Summary and Conclusion

The limited numerical results presented in Section 4 demonstrate that a Monte Carlo procedure developed previously to study a grand canonical ensemble of molecules confined to nodes of a regular lattice and interacting pairwise with finite *attractions* can be extended in a simple way for application to a class of lattice models in which the pair interaction is an infinite *repulsion*. Parameters for the calculation include lattice type and dimensionality, the boundary conditions, the size (i.e., the number of lattice sites, B) and shape of the lattice, the maximum order Q of neighbors excluded by the molecular hard core, and the combination $\beta\mu$ where $\beta = (kT)^{-1}$ and μ is the chemical potential per molecule. In this study we have considered only the two-dimensional triangular lattice with periodic boundary conditions for $Q = 1, 2$, and 3. The size and shape were chosen appropriately for each Q so that when the maximum possible number of molecules (i.e., N_M, which depends on B, Q, and the shape) is placed on the basic lattice, its periodic repetition generates an infinite regular close-packed configuration.

This investigation has also given some evidence for phase transitions. For $Q = 1$, nothing is observed in any of the results which can be considered indicative of a first-order transition, but there is an instability which was subsequently identified by other investigators [19, 20] as a "second-order" transition with an infinite isothermal compressibility at the transition point. It is doubtful that Monte Carlo studies are very useful for studying this type of transition. Assuming this transition is indeed "second-order", the fact that no first-order behavior is

observed offers some reassurance that the Monte Carlo method *can* detect the difference between a first-order transition and one of higher order. The most interesting qualitative result arising from these calculations is the appearance of a possible first-order transition for $Q = 2$, in agreement with Orban and Bellemans' study [21]. The second-neighbor hard-core lattice gas provides a much simpler model than hard discs for investigating the first-order "fluid-solid" transition which appears to be associated with the repulsive part of intermolecular potentials and as such may be more amenable to analytic solution.

Although the appearance of a first-order transition at $Q = 2$, if it is real, leads one to expect no further pronounced qualitative changes for increasing Q, larger values of Q should be considered both to furnish additional insight into the nature of this transition and to help judge its quantitative relevance to the continuum gas of hard discs. Unfortunately, the Markov chain sampling procedure outlined in Section 3 becomes considerably less efficient at $\beta\mu \approx 3$ as Q increases and breaks down completely at about this point for $Q = 3$. No transition was observed for this model with $\beta\mu \leqslant 3$ but an heuristic argument based on scaling the lattice results to agree more closely with discs indicates that the transition may occur considerably above this point, again in agreement with Orban and Bellemans [21]. The techniques they and others have developed since about 1965 seem to be generally more powerful than Monte Carlo methods for studying these models.

ACKNOWLEDGMENTS

It is with lingering sorrow over his tragically early death that I acknowledge the many contributions of Professor Z. W. Salsburg. I shall miss him as a friend, teacher, and colleague; the gap left by his death will never be filled. His specific contributions to this study included some early discussions on the feasibility of adapting the grand ensemble Monte Carlo technique to the study of hard-core lattice models, as well as imparting to me some of his fascination with the properties of the hard disc model and phase transitions in general. The cumulative impact he has had on my thinking is roughly indicated by the number of references I have given to his papers. Professor Salsburg also supplied funds through his National Aeronautics and Space Administration Grant NSG6-59 for computer-related expenses and for my own partial support, for which I am grateful. He also read an early draft of this paper, some years ago, and suggested several revisions to clarify the presentation. Without doubt, the final version could have been substantially improved had his further criticism been possible.

I would also like to thank Mr. Forrest Baskett for writing several of the computer programs, especially the oscilloscope display and magnetic tape systems, and for supervising some of the calculations.

I am also grateful to Shell Development Company for a leave of absence during part of 1964 and 1965, which I spent at the Lawrence Radiation Laboratory in Livermore, California. The first draft of this paper was written during part of my stay there, and I appreciate both the hospitality extended by Lawrence Radiation Laboratory and the many stimulating discussions on the theory of phase transitions I had with Dr. W. G. Hoover, Dr. F. H. Ree, Dr. Ted Einwohner, and Dr. B. J. Alder.

My thanks also go to Shell Oil Company's Rocky Mountain Production Division for permission to publish this study, to Bill Versteeg for his excellent drafting, and to Theodora Mayes, JoAnn Workman, Marsha Jent, and Connie Hooper for their competent and fast typing of the manuscript.

Finally, I thank Professor L. K. Runnels, Professor Andre Bellemans, Professor M. E. Fisher, and Dr. D. S. Gaunt for sending results of their research before publication and for stimulating correspondence and conversation.

REFERENCES

1. N. A. METROPOLIS, A. W. ROSENBLUTH, M. N. ROSENBLUTH, A. H. TELLER, AND E. TELLER, *J. Chem. Phys.* **21** (1953), 1087.
2. M. N. ROSENBLUTH AND A. W. ROSENBLUTH, *J. Chem. Phys.* **22** (1954), 881.
3. W. W. WOOD AND J. D. JACOBSON, *J. Chem. Phys.* **27** (1957), 1207.
4. W. W. WOOD, F. R. PARKER, AND J. D. JACOBSON, *Nuovo Cimento Suppl.* **9** (1958), 133.
5. W. W. WOOD AND J. D. JACOBSON, "Proceedings of the Western Joint Computer Conference, San Francisco," p. 261, Institute of Radio Engineers, New York, 1959.
6. W. W. WOOD, Los Alamos Scientific Laboratory Rept. LA-2827 (1962).
7. E. B. SMITH AND K. R. LEA, *Trans. Faraday Soc.* **59** (1963), 1535.
8. A. ROTENBERG, *J. Chem. Phys.* **42** (1965), 1126.
9. A. ROTENBERG, *J. Chem. Phys.* **43** (1965), 1198.
10. A. ROTENBERG, *J. Chem. Phys.* **43** (1965), 4377.
11. W. W. WOOD, "The Physics of Simple Liquids" (H. N. V. Temperley, J. S. Rowlinson, and G. S. Rushbrooke, Eds), Chap. 5, North Holland, Amsterdam, The Netherlands, 1968.
12. B. J. ALDER AND T. E. WAINWRIGHT, *J. Chem. Phys.* **27** (1957), 1208.
13. B. J. ALDER AND T. E. WAINWRIGHT, *J. Chem. Phys.* **33** (1960), 1439.
14. B. J. ALDER AND T. E. WAINWRIGHT, *Phys. Rev.* **127** (1962), 359.
15. W. G. HOOVER AND B. J. ALDER, *J. Chem. Phys.* **46** (1967), 686.
16. W. G. HOOVER AND F. H. REE, *J. Chem. Phys.* **47** (1967), 4873.
17. B. J. ALDER, *J. Chem. Phys.* **40** (1964), 2724.
18. B. J. ALDER AND W. G. HOOVER, see Ref. [11], Chap. 4.
19. D. S. GAUNT, *J. Chem. Phys.* **43** (1967), 3237.
20. L. K. RUNNELS AND L. L. COMBS, *J. Chem. Phys.* **45** (1966), 2482.
21. J. ORBAN AND A. BELLEMANS, *J. Chem. Phys.* **49** (1968), 363.
22. Z. W. SALSBURG, J. D. JACOBSON, W. FICKETT, AND W. W. WOOD, *J. Chem. Phys.* **30** (1959), 65.
23. J. R. EHRMAN, L. D. FOSDICK, AND D. C. HANDSCOMB, *J. Math. Phys.* **1** (1960), 547.
24. C. P. YANG, IBM Research Rept. RC-564 (1961).
25. D. A. CHESNUT AND Z. W. SALSBURG, *J. Chem. Phys.* **38** (1963), 2861.
26. D. A. CHESNUT, *J. Chem. Phys.* **39** (1963), 2081.
27. T. L. HILL, "Statistical Mechanics," Chap. 8, McGraw-Hill Book Company, New York, 1956.
28. W. W. WOOD AND F. R. PARKER, *J. Chem. Phys.* **27** (1957), 720.
29. J. E. MAYER AND W. W. WOOD, *J. Chem. Phys.* **42** (1965), 4268.
30. O. T. TAUSSKY AND J. TODD, "Symposium on Monte Carlo Methods" (H. A. Meyer, Ed.), p. 15., John Wiley, New York, 1956.

31. B. F. GREEN, JR., J. E. K. SMITH, AND L. KLEM, *J. Assoc. Comput. Machinery* **6** (1959), 527.
32. D. M. BURLEY, *Proc. Phys. Soc. (London)* **85** (1965), 1173.
33. D. S. GAUNT AND M. E. FISHER, *J. Chem. Phys.* **43** (1965), 2840.
34. F. H. REE AND D. A. CHESNUT, *J. Chem. Phys.* **45** (1966), 3893.
35. L. K. RUNNELS, *Phys. Rev. Letters* **15** (1965), 581.
36. M. E. FISHER, *J. Math. Phys.* **4** (1963), 278.
37. L. VAN HOVE, *Physica* **15** (1949), 951.
38. T. L. HILL, "Statistical Mechanics," Appendix 9, McGraw-Hill, New York, 1956.